

NASA/CR—2003-212084



# Convective Array Cooling for a Solar Powered Aircraft

Anthony J. Colozza  
Analex Corporation, Brook Park, Ohio

---

January 2003

## The NASA STI Program Office . . . in Profile

Since its founding, NASA has been dedicated to the advancement of aeronautics and space science. The NASA Scientific and Technical Information (STI) Program Office plays a key part in helping NASA maintain this important role.

The NASA STI Program Office is operated by Langley Research Center, the Lead Center for NASA's scientific and technical information. The NASA STI Program Office provides access to the NASA STI Database, the largest collection of aeronautical and space science STI in the world. The Program Office is also NASA's institutional mechanism for disseminating the results of its research and development activities. These results are published by NASA in the NASA STI Report Series, which includes the following report types:

- **TECHNICAL PUBLICATION.** Reports of completed research or a major significant phase of research that present the results of NASA programs and include extensive data or theoretical analysis. Includes compilations of significant scientific and technical data and information deemed to be of continuing reference value. NASA's counterpart of peer-reviewed formal professional papers but has less stringent limitations on manuscript length and extent of graphic presentations.
- **TECHNICAL MEMORANDUM.** Scientific and technical findings that are preliminary or of specialized interest, e.g., quick release reports, working papers, and bibliographies that contain minimal annotation. Does not contain extensive analysis.
- **CONTRACTOR REPORT.** Scientific and technical findings by NASA-sponsored contractors and grantees.

- **CONFERENCE PUBLICATION.** Collected papers from scientific and technical conferences, symposia, seminars, or other meetings sponsored or cosponsored by NASA.
- **SPECIAL PUBLICATION.** Scientific, technical, or historical information from NASA programs, projects, and missions, often concerned with subjects having substantial public interest.
- **TECHNICAL TRANSLATION.** English-language translations of foreign scientific and technical material pertinent to NASA's mission.

Specialized services that complement the STI Program Office's diverse offerings include creating custom thesauri, building customized databases, organizing and publishing research results . . . even providing videos.

For more information about the NASA STI Program Office, see the following:

- Access the NASA STI Program Home Page at <http://www.sti.nasa.gov>
- E-mail your question via the Internet to [help@sti.nasa.gov](mailto:help@sti.nasa.gov)
- Fax your question to the NASA Access Help Desk at 301-621-0134
- Telephone the NASA Access Help Desk at 301-621-0390
- Write to:  
NASA Access Help Desk  
NASA Center for Aerospace Information  
7121 Standard Drive  
Hanover, MD 21076

NASA/CR—2003-212084



# Convective Array Cooling for a Solar Powered Aircraft

Anthony J. Colozza  
Analex Corporation, Brook Park, Ohio

Prepared under Contract NAS3-00145

National Aeronautics and  
Space Administration

Glenn Research Center

---

January 2003

The Propulsion and Power Program at  
NASA Glenn Research Center sponsored this work.

Available from

NASA Center for Aerospace Information  
7121 Standard Drive  
Hanover, MD 21076

National Technical Information Service  
5285 Port Royal Road  
Springfield, VA 22100

Available electronically at <http://gltrs.grc.nasa.gov>

# Convective Array Cooling for a Solar Powered Aircraft

Anthony J. Colozza  
Analex Corporation  
Brook Park, Ohio 44142

## Introduction and Background

The ability to fly an unmanned aircraft under solar power has been demonstrated.<sup>1,2</sup> The uniqueness of a solar powered aircraft, compared to a conventionally powered aircraft, lends its use to equally unique applications both military and civilian. Most of these applications involve subsonic flight at either high altitudes or for long durations or both. The advantages of solar power over conventionally powered fuel burning propulsion systems, for these types of applications, is that a solar power system does not require the use of the atmosphere in the generation of power. This eliminates the need for multiple stage compressors that are necessary for high altitude combustion driven aircraft. Also since the power for flight comes from the sun, no fuel supply is needed. If this solar system is coupled to a regenerative fuel cell system or rechargeable battery system of sufficient energy density (approximately 400 Wh/kg or greater) then long endurance flight on the order of weeks to months can be achieved depending on the flight location.<sup>3-5</sup>

Since the available power for the aircraft is limited by the solar flux from the sun (approximately 1000 W/m<sup>2</sup>) any increase in the ability to utilize this available power is beneficial to the aircraft's performance. State-of-the-art production solar cells operate in the range of approximately 10 to 20 percent efficiency, depending on the type of solar cell and its operating temperature. By increasing the efficiency of the solar cells on a given aircraft, significant performance enhancements for the aircraft can be achieved. This can enable the aircraft to perform missions previously not possible. The increased capability in both mission duration, achievable altitude and location can be seen in Figure 1. This figure compares the maximum achievable altitude, at a given latitude, for the same solar aircraft with 14 and 18 percent efficient solar cells. The 14 percent solar cell efficiency was selected because it represents what is achievable with present day silicon solar cells. The 18 percent efficiency is an estimate of what can be achieved utilizing the same type of solar cells but having them operate at a lower temperature. The data is plotted for two dates, June 21st (summer solstice) and December 21st (winter solstice). These two dates represent the longest and shortest days, respectively, for the year. Maximum altitude curves for any other date should fall somewhere between these two sets of curves. From this figure it can be seen that the capabilities of the solar aircraft increase with increasing solar cell efficiency. An example of enhanced mission capability can be shown by examining the highest altitude that can be achieved for a specific latitude. For a maximum altitude of 20 km on December 21st, the highest flight latitude increases from 25° to 34° with an increase in cell efficiency from 14 to 18 percent. This represents a 34 percent increase in possible flight latitudes, which greatly enhances the aircraft's mission capabilities. These and other benefits are also shown in References 3, 4 and 5.

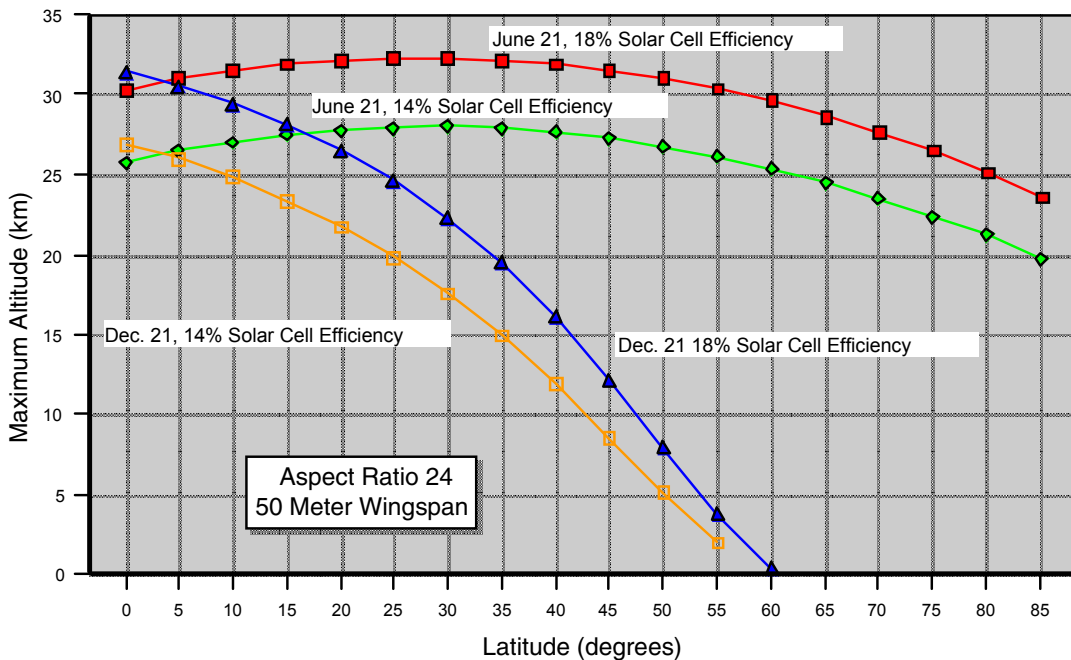


Figure 1.—Effect of Increase In Solar Cell Efficiency on Aircraft Performance.

In order to achieve a lower solar cell operating temperature, it has been suggested that the wing of a solar powered aircraft with an integral thermal control system can be used to take advantage of the airflow over the wing to assist in cooling the solar cells. The concept, shown in Figure 2, directs a small amount of air through a duct in the wing to convectively cool the backside of the solar cells. This is an additional heat transfer mechanism, which adds to convective and radiative cooling of the solar cells from the topside. This additional heat transfer mechanism can significantly reduce the operating temperature of the solar cells, thereby improving their efficiency, and it may be possible to achieve this with little or no detrimental aerodynamic drag.

The relationship between solar cell efficiency and temperature has been well documented. This effect is consistent for all types of solar cells. Most solar arrays do not have active cooling incorporated into the array design. This is because adequate cooling can most often be obtained by using the large area on the backside of the solar array as a waste heat radiator. An additional increase in the efficiency of the solar cells could be achieved by incorporating a cooling system to enhance heat dissipation; however, in almost all applications, the cost, complexity and added mass make this undesirable. Therefore little research has been done on arrays that have airflow passages for convective cooling. However, in an application such as a solar powered aircraft, in which an air stream of cold air is readily available, the benefits of convective cooling can be substantial. By reducing the temperature of the solar cells, a significant increase in solar cell efficiency can be achieved. For example, a typical commercial silicon solar cell

efficiency will increase from 13 to 17 percent when cooled from 25 to  $-25^{\circ}\text{C}$ . This translates into a 30 percent increase in performance. The change in efficiency with temperature for various types of solar cells is shown in Figure 3.<sup>6</sup> A strong trend of increasing efficiency with temperature is shown for six different types of solar cells. As temperature goes down, efficiency improves dramatically. It is estimated that this increase in cell efficiency can reduce the size of the aircraft or increase the available power with little impact on the weight or size of the aircraft.

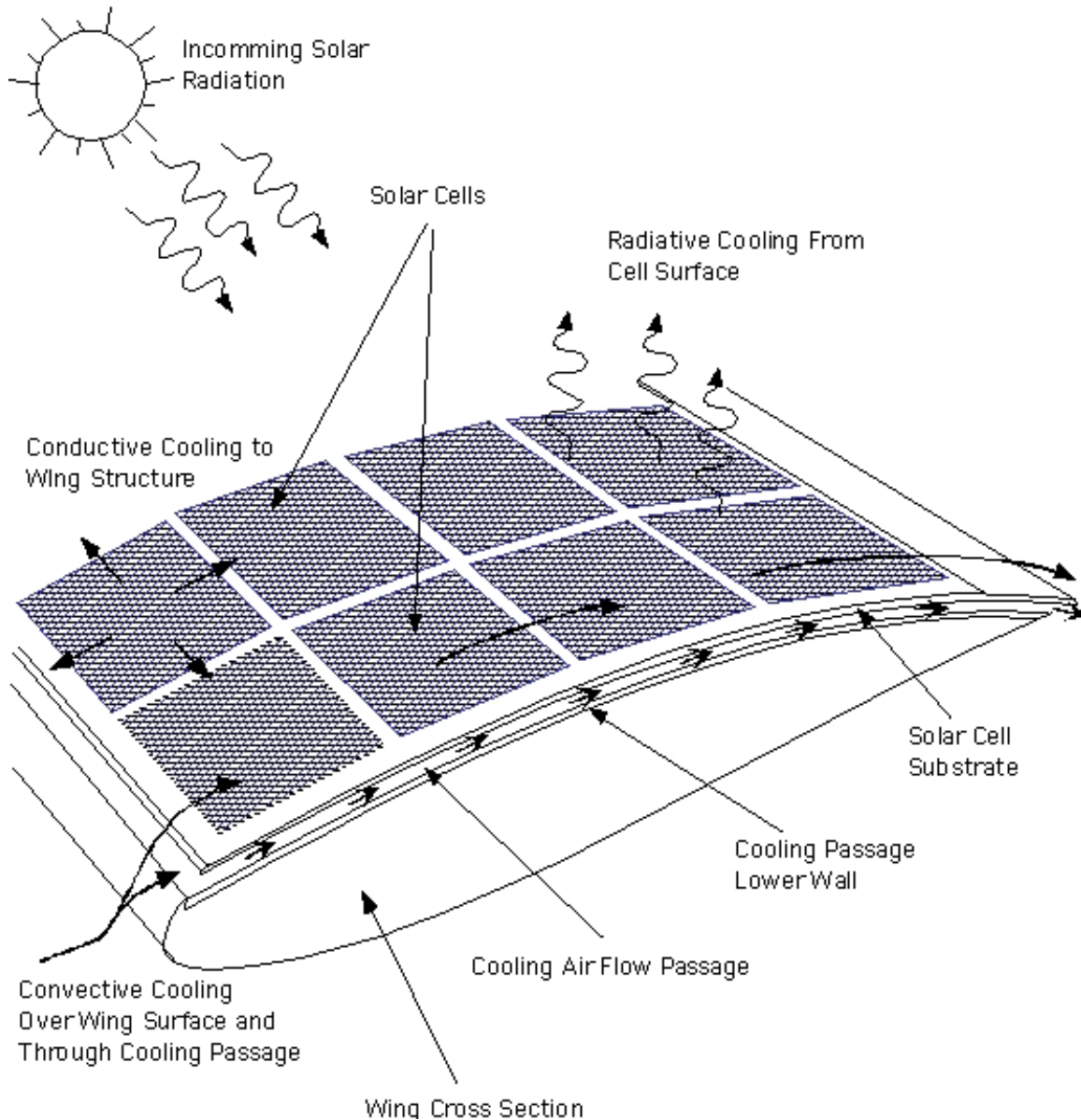


Figure 2.—Heat Transfer Mechanisms for a Solar Array with Integral Cooling Passage.

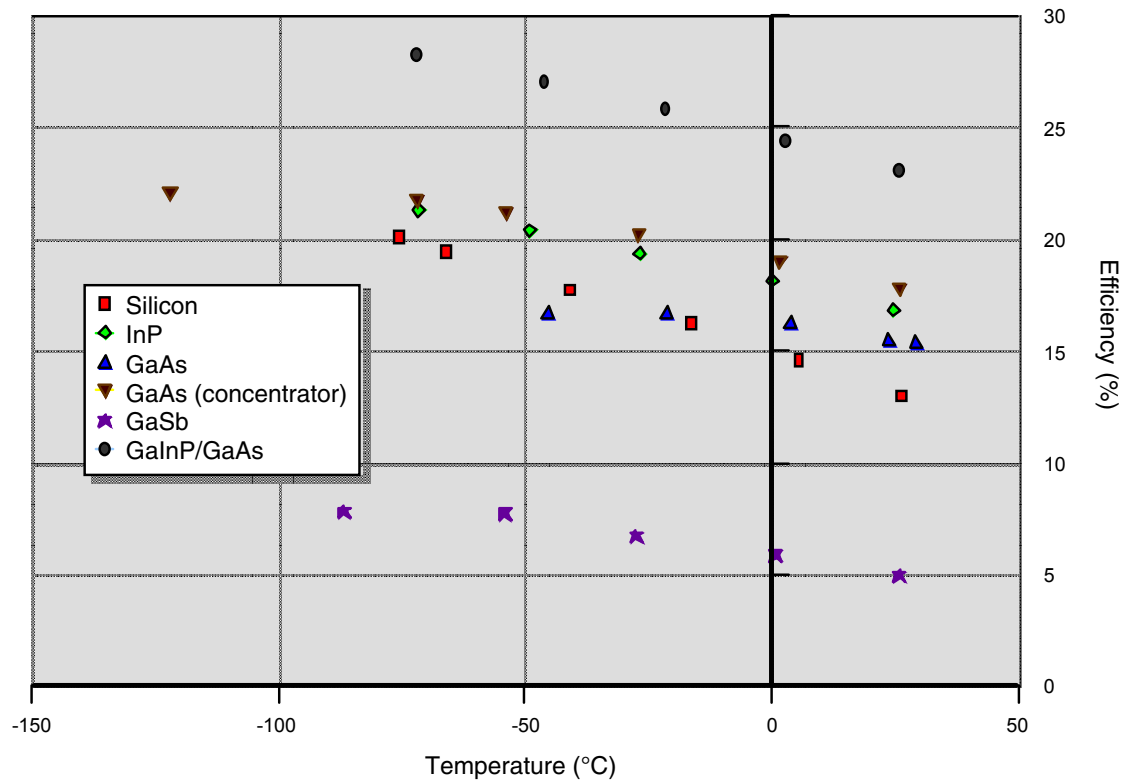


Figure 3.—Effect of Temperature on Efficiency of Various Types of Solar Cells.<sup>6</sup>

### Preliminary Analysis

It is a well understood principle that the operating efficiency of a solar cell is directly related to its operating temperature. The proposed concept is based on the ability to reduce the operating temperature of the solar cells by circulating low temperature air, available at flight altitudes, underneath the solar cells thereby cooling them. In order for this concept to be feasible and practical for use in an aircraft, it must be shown that, by circulating air underneath the solar cells, their operating temperature can be lowered enough to produce a justifiable increase in efficiency without affecting the performance of the aircraft. A preliminary analysis has been performed and is outlined below. This analysis was done to establish the feasibility of the concept and to estimate the performance increase that may be achieved. Figure 2 shows the proposed concept and the heat transfer mechanisms involved in establishing the solar cell temperature. The energy balance for the solar cells (energy in,  $E_{in}$ , is equal to energy out,  $E_{out}$ ) and subsequent heat balance is given by the following equations where  $Q_{solar}$  is the heat input from the incident solar radiation falling on the solar cells,  $Q_{conduction}$  is the heat transferred from the solar cells by conduction to the surrounding aircraft,  $Q_{convection}$  is the heat transferred from the solar cells by convection to the air stream,  $Q_{radiation}$  is the heat transferred from the solar cells by radiation to the surroundings and  $Q_{electric}$  is the electrical power produced by solar cells.



$$E_{in} = E_{out} \quad (1)$$

$$Q_{solar} = Q_{conduction} + Q_{convection} + Q_{radiation} + Q_{electric} \quad (2)$$

The input solar radiation on a clear day can be assumed to be approximately 1000 W/m<sup>2</sup> and assuming a 15 percent efficient solar cell the output power (P<sub>out</sub>) would be 150 W/m<sup>2</sup>. Based on an operating temperature of approximately 20 to 30 °C, for a solar cell installed on the wing of an aircraft, the main heat transfer mechanism will be the convective cooling over the wing surface. Therefore combining the radiative and conductive heat transfer terms together and calling them Q<sub>secondary</sub> the heat transfer equation becomes;

$$850 \text{ (W/m}^2\text{)} = Q_{convection} + Q_{secondary} \quad (3)$$

The convective heat transfer term is based on the solar cell temperature (T), the surrounding atmospheric temperature (T<sub>a</sub>) and the convective heat transfer coefficient (h<sub>1</sub>).

$$Q_{convection} = h_1(T - T_a) \quad (4)$$

Some assumptions must be made about the aircraft and its flight conditions. These assumptions are based on typical missions and flight conditions for a high altitude unmanned solar powered aircraft.

Flight Altitude	18 km
Flight Velocity (U)	0.1 Mach
Wing Chord (c)	1 m

The convective heat transfer coefficient over the surface of the wing can be estimated as follows. The Reynolds number based on chord (Re<sub>l</sub>) length is given by;

$$Re_l = U_{FreeStream} \frac{L}{\mu} \quad (5)$$

where:

Free Stream Velocity, U <sub>free stream</sub> :	30 (m/s)
Wing Chord Length, L:	1 (m)
Viscosity, μ:	1.165E-4 (m <sup>2</sup> /s)

This produces a Reynolds number of 257,510. Since this Reynolds number value is less than 500,000 it can be assumed that the flow is laminar over the wing surface. For laminar flow, the Nusselt number based on chord length (Nu<sub>l</sub>) is given by Equation 6.<sup>7</sup>

$$Nu_l = 0.664 Re_l^{1/2} Pr^{1/3} \quad (6)$$

where the Prandtl number (Pr) is given by the following equation.

$$\text{Pr} = \frac{c_p m}{k} \quad (7)$$

Constant Pressure Specific Heat of Air,  $c_p = 1.006$  (KJ/Kg °K)  
 Air Mass Flow,  $m = 1.422\text{E-}5$  (Kg/m s)  
 Thermal Conductivity of Air,  $k = 0.0195$  (W/m °K)

Using these values  $\text{Pr} = 0.734$  and  $\text{Nu}_1 = 303.95$  the heat transfer coefficient for the surface of the wing,  $h_1$ , is given by the following equation, where  $c$  is the wing chord length.

$$h_1 = \frac{\text{Nu}k}{c} = 5.927 \left( \frac{W}{m^2 \text{ } ^\circ K} \right) \quad (8)$$

Based on previous experience and tests conducted at the NASA Glenn Research Center the operating temperature of a solar cell in a sealed wing under  $1000 \text{ W/m}^2$  illumination can be estimated to be  $293 \text{ } ^\circ K$ .<sup>8,9</sup> Based on this information, Equation 3 can be used to estimate the heat transfer due to the secondary mechanisms. Substituting in the values determined above into this equation yields;

$$850 = 5.927 (293 \text{ } ^\circ K - 216 \text{ } ^\circ K) + Q_{\text{secondary}} \quad (9)$$

Solving for  $Q_{\text{secondary}}$  yields

$$Q_{\text{secondary}} = 394 \text{ W/m}^2 \quad (10)$$

Now by adding a convective cooling passage within the wing a second convective heat transfer path is obtained. The convective heat transfer coefficient ( $h_2$ ) for this second path must now be determined. The Reynolds number for this passage, based on the passage wall spacing ( $d$ ), is given by the following equation where  $\nu$  ( $\text{m}^2/\text{s}$ ) is the kinematic viscosity of air.

$$\text{Re}_d = U \frac{d}{\nu} \quad (11)$$

Using a passage wall spacing of  $0.009 \text{ m}$  yields a Reynolds number of approximately  $2300$ . This value of Reynolds number is just at the edge of transition from laminar to turbulent for flow between parallel plates therefore it can be assume that the flow is laminar. For laminar flow in a rectangular duct with an infinite aspect ratio, the Nusselt number has a value of  $8.23$ . The equation for Nusselt number based on the passage wall spacing ( $\text{Nu}_d$ ) is given in Equation 12.<sup>7</sup>

$$\text{Nu}_d = h_2 \frac{d}{k} = 8.23 \quad (12)$$

This equation can be solved for  $h_2$  by substituting in the values for the remaining parameters.

$$h_2 = \frac{(8.23)(0.0195)}{(0.009)} = 17.83 \left( \frac{W}{m^2 \cdot K} \right) \quad (13)$$

Since the actual value of  $Q_{\text{secondary}}$  for an array utilizing the cooling passage is not known, the cell temperature with the cooling passage can be calculated for both extremes, when  $Q_{\text{secondary}}$  is equal to the value without the cooling passage and when  $Q_{\text{secondary}}$  is equal to zero. The actual cell temperature will lie somewhere between these extremes. For the first case, using the value of  $Q_{\text{secondary}}$  given in Equation 9 and the calculated convective heat transfer coefficients,  $h_1$  and  $h_2$ , the temperature of the solar cells is given by the following equation.

$$850 = 5.927 (T - 216 \text{ }^\circ\text{K}) + 17.83(T - 216 \text{ }^\circ\text{K}) + 394 \quad (14)$$

Solving this for the solar cell temperature,  $T$ , yields;

$$T = 235 \text{ }^\circ\text{K} \quad (15)$$

To bound the problem the temperature when  $Q_{\text{secondary}}$  is equal to zero is calculated by the following equation.

$$850 = 5.927 (T - 216 \text{ }^\circ\text{K}) + 17.83(T - 216 \text{ }^\circ\text{K}) \quad (16)$$

Solving for the solar cell temperature,  $T$ , yields:

$$T = 252 \text{ }^\circ\text{K} \quad (17)$$

The actual solar cell temperature will lie somewhere between these two extremes. It is this actual temperature that will be determined through a more thorough analysis in the following section. For the purposes of this preliminary analysis the average of these two temperature extremes, 243 °K, will be assumed to be the resulting solar cell temperature.

Comparing this temperature to that estimated for the solar cell array with no cooling passage yields:

$$\Delta T = 298 \text{ }^\circ\text{K} - 243 \text{ }^\circ\text{K} = 55 \text{ }^\circ\text{K} \quad (18)$$

This  $\Delta T$  value represents a significant drop in the temperature of the solar cells compared to their temperature when no cooling passage is used. The effect of this temperature drop on the performance of the solar cells can be determined from the data given in Figure 2. For silicon solar cells, the change in efficiency corresponding to this  $\Delta T$  is approximately 3.5 percent. This translates into an estimated increase in cell performance of 25 percent.

This preliminary analysis demonstrates the feasibility of using a cooling passage to significantly reduce the solar cell temperature and thereby increase its efficiency. The next main feasibility issue is to assess the effect this cooling passage will have on the performance of the aircraft. This can be done by calculating the pressure drop in the cooling passage and determining the corresponding drag.

The Reynolds number for the flow through the cooling passage was given above as 2300. The friction factor for laminar flow between parallel plates ( $f_{lam}$ ) is given by the following equation.<sup>10</sup>

$$f_{lam} = 96/Re_d = 0.0417 \quad (19)$$

The pressure drop in the cooling passage ( $\Delta P$ ) is given by the following equation. Where  $\rho$  is the air density at altitude,<sup>13</sup>  $d$  is the passage spacing (0.009 m),  $U$  is the free stream velocity (30 m/s) and  $L$  is the wing chord length (1 m).

$$\Delta P = \rho f_{lam} L U^2/8d \quad (20)$$

substituting the values for the variables yields

$$\Delta P = 63.6 \text{ Pa} \quad (21)$$

For a wingspan of 20 m, assuming the cooling passage extends the length of the wing, the frontal area ( $A_f$ ) of the cooling passage is  $0.18 \text{ m}^2$ . This area yields a drag ( $D$ ) of:

$$D = \Delta P A_f = (63.6)(0.18) = 11.45 \text{ N} \quad (22)$$

The total drag of a similarly sized, aerodynamically clean aircraft at similar flight conditions without the cooling passage would be approximately 150 N. This translates into a 7 percent increase in the drag of the aircraft. Comparing the drag increase of 7 percent to the increase in solar cell performance of 25 percent indicates that, based on this preliminary analysis, this concept will have beneficial effects on the performance of the aircraft.

## Detailed Analysis

Based on the preliminary results, a more detailed analysis was warranted in order to fully evaluate this concept. A computer-based analytical model of the solar array with a cooling passage was developed. This model takes into account the heat transfer from the solar cells to the surroundings and the fluid flow over the cells and through the cooling passage. The heat transfer analysis was accomplished by setting up an energy balance including radiative and convective heat transfer mechanisms. Since it was assumed that the solar cells were isolated from the aircraft structure, the conductive heat transfer path was assumed to be minimal and therefore not included in the analysis.

$$\text{Solar Flux Into Solar Cells} = \text{Heat Transfer Out of Solar Cells} + \text{Electrical Energy Produced} \quad (23)$$

This analysis was used to predict the temperature of each solar cell along a cross section of the wing chord and determine its corresponding output power. This analysis takes into account the variation in electrical power output of the array as a function of temperature and the variation of input power from the sun, as a function of the day of the year, location and time of day. An example of this variation is shown in Figure 4. The analytical model was then used to optimize the array cooling passage in order to produce the greatest output power for given flight conditions and to keep the drag produced by the cooling passage to a minimum. The main issues examined through this analysis are the change in output power of the array due to the addition of the cooling passage and the drag produced by the cooling passage.

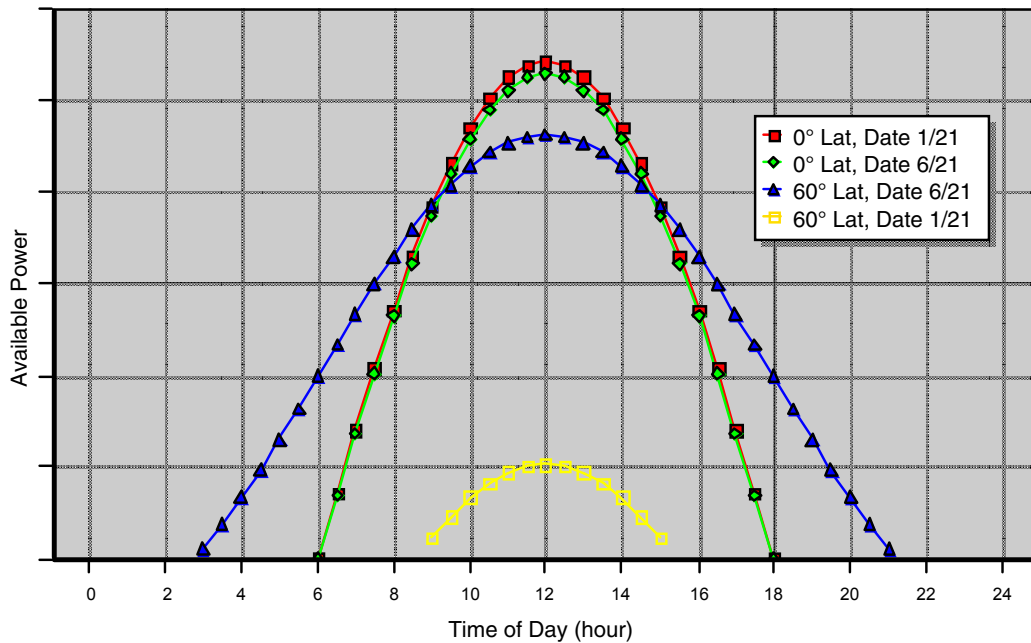


Figure 4.—Available Power Curves for Various Location and Date Combination.

The computer code, which was developed through this modeling process, utilizes various inputs that represent the configuration of the array and wing section and flight conditions to determine the desired quantities such as cell temperature, output power and drag. This analysis was done through an iterative process. A diagram of the proposed computer code logic is shown in the flow chart given in Figure 5. The ability to model the array under various conditions and configurations is necessary in order to provide a clear indication as to the benefits of the integral air-cooling passage on the solar cell performance. The following is a brief description of the analysis that was performed.

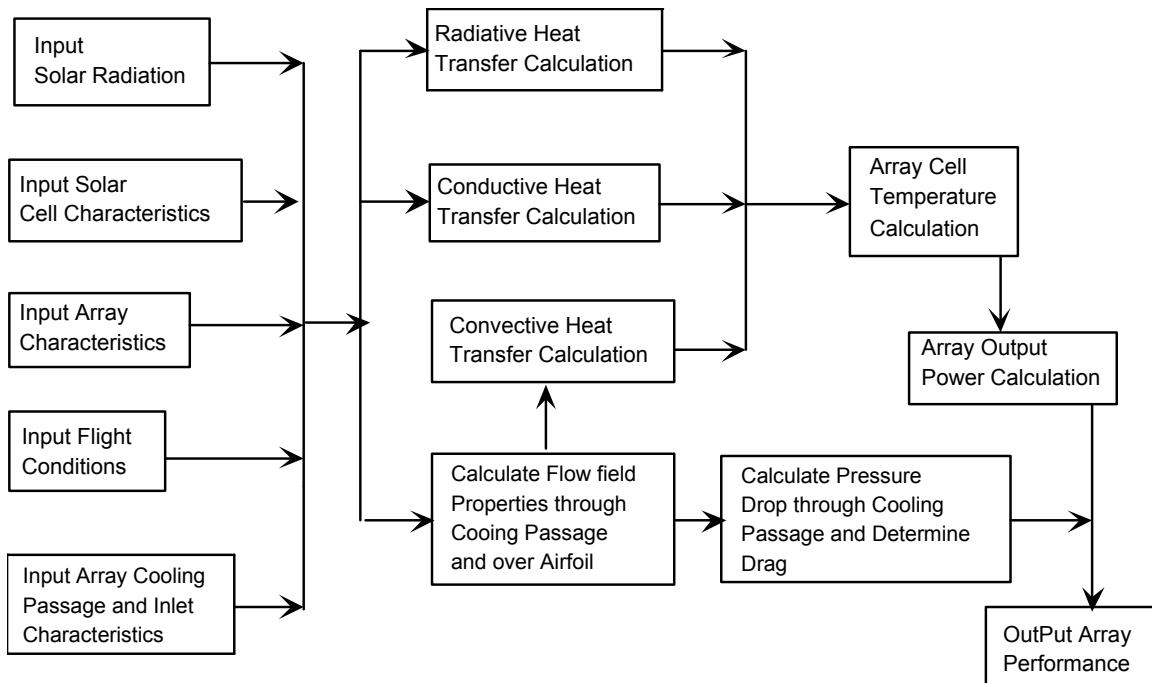


Figure 5.—Computer Code Analysis Flow Chart.

The first step in determining the cell performance is to calculate the incoming solar flux and incident angle of the solar radiation on the solar cell as well as the amount of this energy reflected off of the cell. The solar flux (SF), which varies slightly throughout the year, is determined by calculating the actual distance the earth is from the sun,  $r$ , at a selected time of year. This is given by the following equations:

$$r = r_m \frac{(1 - \varepsilon^2)}{(1 + \varepsilon \cos(\alpha))} \quad (24)$$

$$\alpha = \frac{2\pi(n - 4)}{365} \quad (25)$$

$$SF = SF_m \tau \frac{r_m^2}{r^2} \quad (26)$$

Where the mean radius of the earth ( $r_m$ ) is 1.496E8 km, Earth's orbital eccentricity ( $\varepsilon$ ) is 0.017, the mean solar flux at orbit ( $SF_m$ ) is  $1352 \text{ W/m}^{2-4}$  and the day number ( $n$ ) is based on the day of the year (for January 1,  $n = 1$ ). For this analysis the solar attenuation factor due to the atmosphere,  $\tau$ , is assumed to be 0.80.

The incident angle of the incoming solar radiation ( $\theta$ ) on the solar cell is dependent on the solar declination angle ( $\delta$ ), the latitude ( $\phi$ ), the orientation of the solar cell represented by its inclination angle ( $\beta$ ) and azimuth angle ( $\gamma$ ) and the time of day

represented by the hour angle ( $\omega$ ). The equations for determining the incident angle are as follows.<sup>3,4,11</sup>

Earth's declination angle ( $\delta$ ) varies with the day of the year ( $d_n$ ). This day number ( $d_n$ ) is based on the vernal equinox, so  $d_n = 1$  is March 21st.

$$\delta = 0.4091 \sin\left(\frac{2\pi d_n}{365}\right) \quad (27)$$

The hour angle ( $\omega$ ) is given by the following expression, where "i" is the instantaneous time of day in hours. The convention for  $\omega$  is negative before noon, positive after noon and zero at noon.

$$\omega = 2\pi \frac{(i - 11.968)}{23.935} \quad (28)$$

The inclination angle ( $\beta$ ) of the solar cell is dependent on its location on the surface of the airfoil and the length of the individual solar cell ( $l$ ). Since the airfoil is curved, each cell along the chord will be at a different inclination angle. A curve fit of the airfoil upper surface can be used to determine the cell incident angle by calculating the height of the wing surface from the centerline at the beginning and end of each cell. The angle produced with the horizontal based on the difference of these two heights is the inclination angle. The inclination angle of the cells on the front portion of the airfoil will be positive and those on the rear portion will be negative. The determination of the cell angle is illustrated in Figure 6 for a NACA 0009 airfoil. It should be noted that these equations assume that the wing chord centerline is horizontal. If the aircraft is climbing or performing any other maneuver then the deviation of the centerline off of the horizontal must be added (or subtracted) to the inclination angle.

The following equations represent the curve fit for the NACA 0009 upper surface of the airfoil.

$$y = 0.008 + 0.349x - 1.044x^2 + 1.179x^3 - 0.494x^4 \quad (29)$$

$$\beta = \frac{\tan^{-1}(y_a - y_b)}{l} \quad (30)$$

The last angle needed in order to calculate the incidence angle is the azimuth angle ( $\gamma$ ) for the wing. The convention for this angle is zero due South, East is negative and West is positive.  $\gamma$  can have values of  $-\pi$  to  $+\pi$ . The diagram shown in Figure 7 demonstrates the convention for this angle.

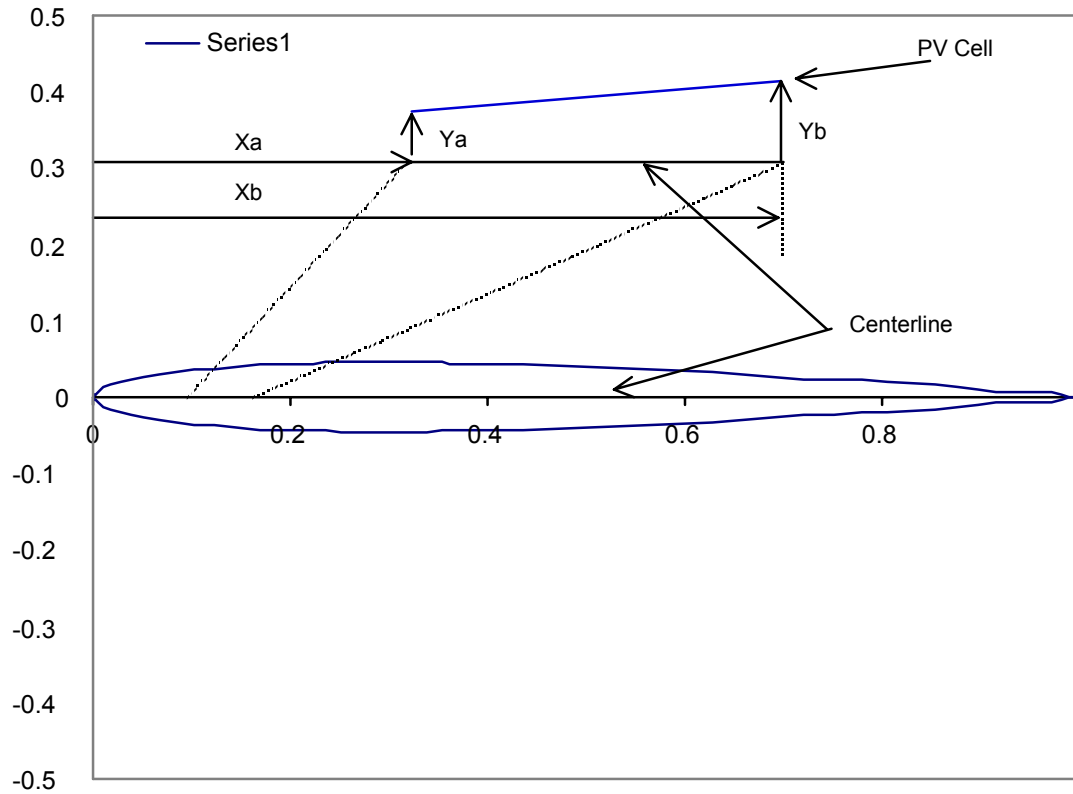


Figure 6.—NACA 0009 Airfoil and PV Cell Coordinate Geometry.

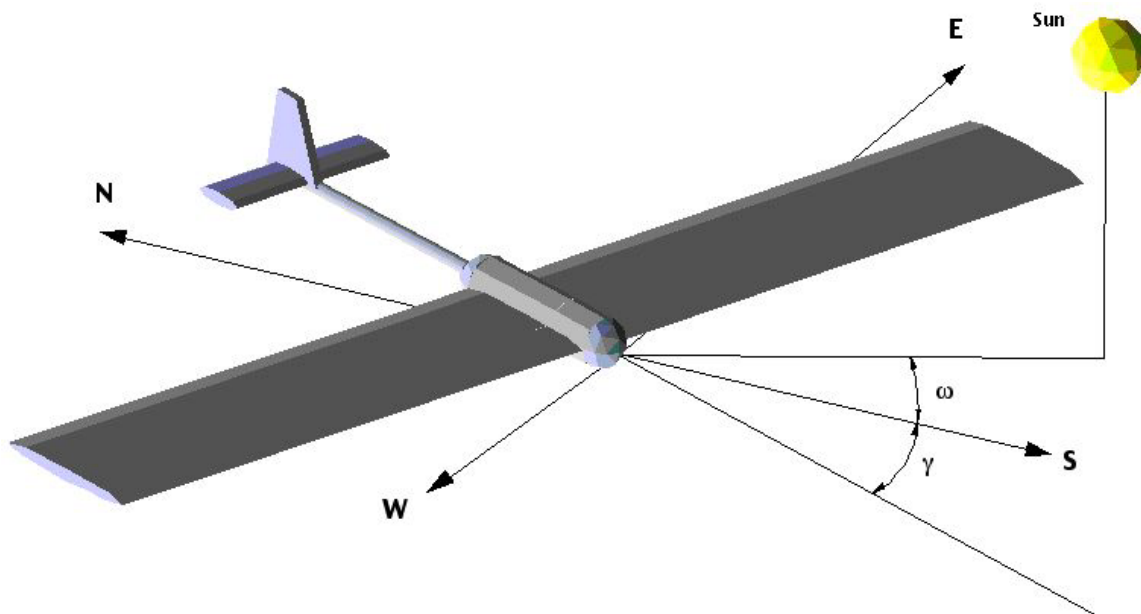


Figure 7.—Coordinate System for Hour Angle ( $\omega$ ) and Azimuth Angle ( $\gamma$ ).



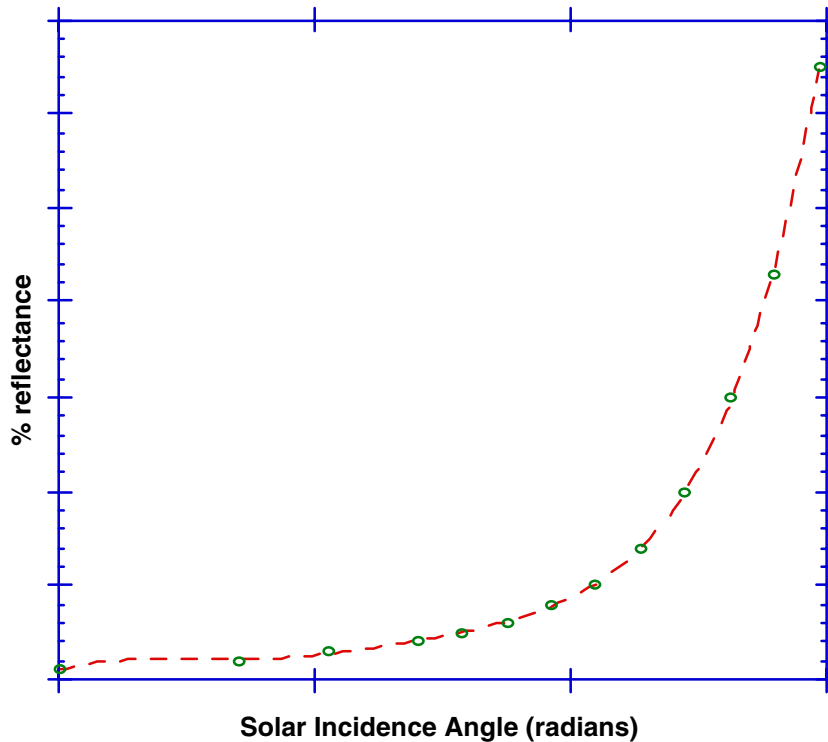


Figure 8.—Reflectance of Solar Radiation as a Function of Incident Angle.

Once the angles described above are determined, the incident angle of a given cell can be calculated by the following relationship.<sup>12</sup>

$$\theta = \text{acos}(\sin(\delta) \sin(\phi) \cos(\beta)) - (\sin(\delta) \cos(\phi) \sin(\beta) \cos(\gamma)) + (\cos(\delta) \cos(\phi) \cos(\beta) \cos(\omega)) + (\cos(\delta) \sin(\phi) \sin(\beta) \cos(\gamma) \cos(\omega)) + (\cos(\delta) \sin(\beta) \sin(\gamma) \sin(\omega)) \quad (31)$$

After the inclination angle is known it is now possible to determine the percent of solar energy that is reflected off of the surface of the solar cell. The percent reflectance is based on the type of solar cell material, surface coating and incident angle of the solar radiation. For this analysis the solar cell material was assumed to be Silicon with a VMI antireflection coating. The reflectance for this type of material is shown in Figure 8 and the corresponding curve fit of reflectance (RF) versus incident angle in radians is given in Equation 32.

$$\text{RF} = 0.99031 + 17.1\theta - 91.459\theta^2 + 209.74\theta^3 - 201.52\theta^4 + 73.893\theta^5 \quad (32)$$

Utilizing the above equations to determine the amount of solar energy entering the solar cell, an energy balance on each solar cell can be performed in order to determine its operating temperature. This energy balance is given in Equation 2 where the incoming solar energy ( $Q_{\text{solar}}$ ) can be represented by the following equation.

$$Q_{\text{solar}} = SF (1-RF) \cos(\theta) \quad (33)$$

As mentioned previously, the conduction term ( $Q_{\text{conduction}}$ ) from Equation 2 is assumed to be zero. The remaining terms for output power ( $Q_{\text{electric}}$ ), convection heat transfer ( $Q_{\text{convection}}$ ) and radiation heat transfer ( $Q_{\text{radiation}}$ ) are all dependent on the solar cell temperature ( $T$ ). Therefore the energy balance equation must be solved iteratively for each solar cell along the chord of the wing.

The dependence of the solar cell efficiency and therefore electrical output power on temperature is shown in Figure 9 for a Silicon solar cell. The solar cell efficiency ( $SC_{\text{eff}}$ ) curve as a function of temperature ( $T$ ) shown in Figure 9 is represented by Equation 34.

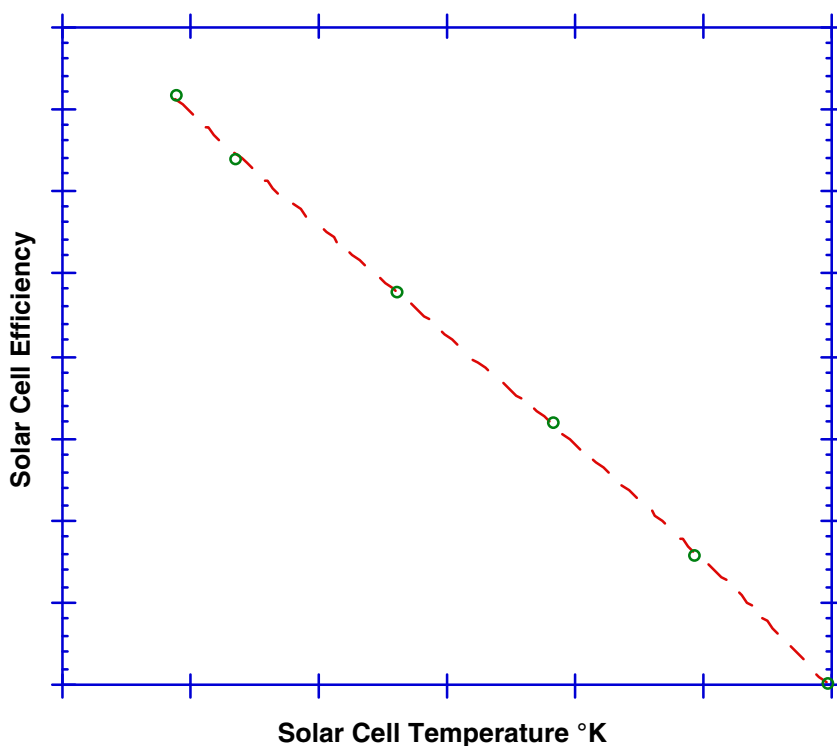


Figure 9.—Silicon Solar Cell Efficiency as a Function of Temperature.

$$SC_{\text{eff}} = 0.55977 - 0.0035564 T + 1.2178e-05 T^2 - 1.7013e-08 T^3 \quad (34)$$

Therefore, based on the above relation for solar cell efficiency, the electrical output of the solar cell can be expressed by Equation 35.

$$Q_{\text{electric}} = SF (1-RF) \cos(\theta) SC_{\text{eff}} \quad (35)$$

The convective heat transfer mechanism can be broken up into two portions; the convective heat transfer over the upper surface of the wing,  $Q_{\text{surface}}$ , and the convective heat transfer through the cooling passage under the solar cells,  $Q_{\text{passage}}$ .

$$Q_{\text{convection}} = Q_{\text{surface}} + Q_{\text{passage}} \quad (36)$$

Where  $Q_{\text{surface}}$  is given by Equations 4 to 8. Since this detailed analysis is being done for a general case, relations for the physical properties of the atmosphere are needed. These can be found in most standard atmosphere texts such as that given in Reference 13. The relations for the air conductivity ( $k$ ) and viscosity ( $\nu$ ) are given below as a function of atmospheric temperature,  $T_a$ .

$$k = \frac{6.325e - 7T_a^{1.5}}{\frac{-12}{(T_a + 24510 T_a) 4186.8}} \quad (37)$$

$$\nu = 2.17e - 5 \left( \frac{T_a}{237} \right)^{0.67} \quad (38)$$

Also, Equation 6 that represents the Nusselt number (Nu), is valid only for Reynolds numbers less than 500,000. For Reynolds numbers (Re) greater than 500,000 the following relation is used.<sup>7</sup>

$$\text{Nu} = (0.037 \text{ Re}^{0.8} - 871) \text{ Pr}^{1/3} \quad (39)$$

The convective heat transfer due to the cooling passage must also be calculated. This heat transfer path is represented by the following equation, where  $T_{ai}$  is the inlet air temperature in the cooling passage at the beginning of a given cell and  $T_{ao}$  is the exit air temperature in the cooling passage for the same cell.

$$Q_{\text{passage}} = \frac{h_2(T_{ai} - T_{ao})}{\log\left(\frac{T - T_{ao}}{T - T_{ai}}\right)} \quad (40)$$

where  $T_{ao}$  is given by the following equation.

$$T_{ao} = T + (T_{ai} - T) e^{-\frac{ch_2}{dU\rho c_p}} \quad (41)$$

The final heat transfer mechanism that must be accounted for is radiation heat transfer from the cell to the surroundings,  $Q_{\text{radiation}}$ . For this analysis it is assumed that the radiation heat transfer takes place between the solar cell and the sky only, no radiation is considered between the solar cells and the aircraft structure. The following equation represents the radiation heat transfer. It is assumed that the emissivity of Silicon ( $\epsilon$ ) is 0.3 and the sky temperature ( $T_{\text{sky}}$ ) is 263 °K. The Boltzman constant ( $\sigma$ ) is  $5.67e-8 \text{ W/m}^2 \text{ }^\circ\text{K}$

$$Q_{\text{radiation}} = \epsilon \sigma (T^4 - T_{\text{sky}}^4) \quad (42)$$

The heat transfer mechanisms described above allow the temperature of each cell to be calculated for a given set of flight conditions and wing geometry. Each cell

temperature is calculated individually along the wing chord. This is necessary since the air temperature within the cooling passage changes as it passes beneath each cell. Utilizing this approach, the input quantities can be varied and the effectiveness of the cooling passage on increasing the aircraft's performance can be determined. The results for the above analysis are given in the following section.

## Results

Based on the analysis method described in the previous section, data was generated to determine the effect of the cooling passage on the power generation capabilities of a high altitude solar powered aircraft. Using a range of variables, the performance of the solar array with the cooling passage was determined for a number of flight conditions. The passage spacing was first optimized by determining the spacing that produced the greatest increase in solar array performance, while minimizing the effect of drag on the aircraft. This was done by generating data on solar cell efficiency and drag per unit wing length versus cooling passage spacing. This is shown in Figure 10. This initial optimization was performed for a set of selected flight conditions and solar cell and airfoil geometry. This base flight configuration was chosen as the flight conditions and geometry from which all variations will be compared. In other words, variations from this initial configuration will be used to determine what impact the variables have on the performance of the cooling passage. The values for the variables in this initial flight configuration are given below in Table 1.

Table 1.—Base Flight Conditions

Solar Cell (Type Size)	Silicon, 6 cm × 6 cm
Airfoil	NACA 0009
Chord Length	1 m
Flight Date	May 21
Flight Latitude	40° North
Aircraft Orientation During Flight (N, S, E, W)	South
Flight Altitude	20 km

Using the data represented in Figure 10 and the performance of the solar array without any cooling passage, the percent change in the solar array output and drag was determined. This is shown in Figure 11. Average cell efficiency without the cooling passage, for the base flight conditions was determined to be 7.3 percent at an operational temperature of 80 °C. Drag for the aircraft was estimated to be approximately 150 N at the flight conditions.

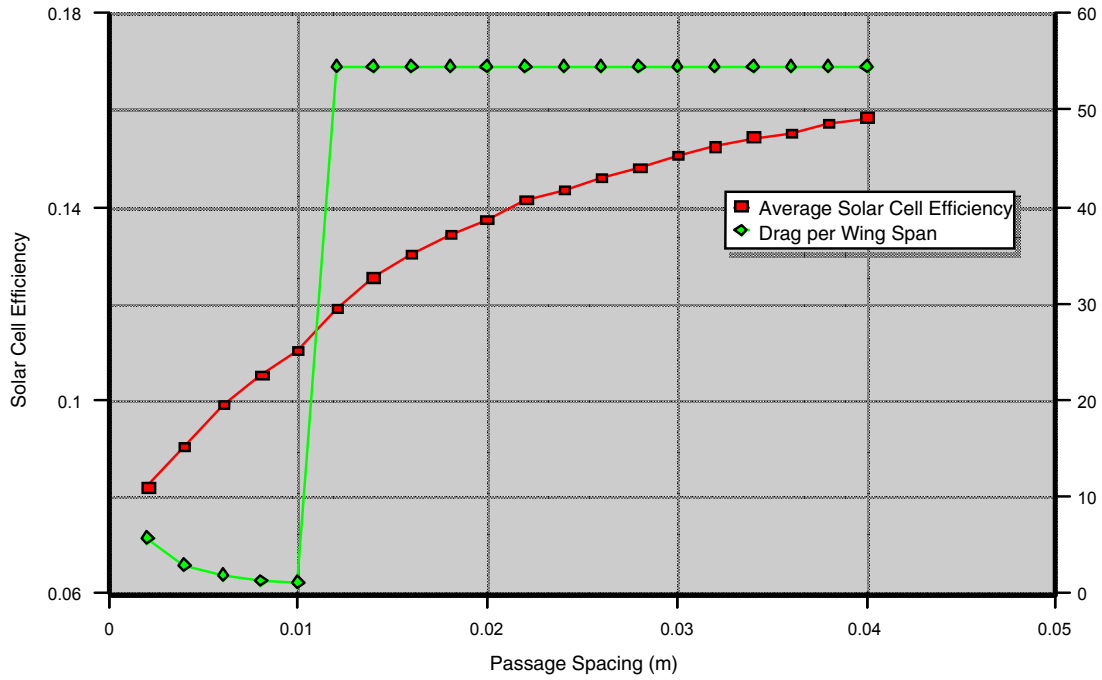


Figure 10.—Effect of Passage Spacing on Solar Cell Efficiency and Drag.

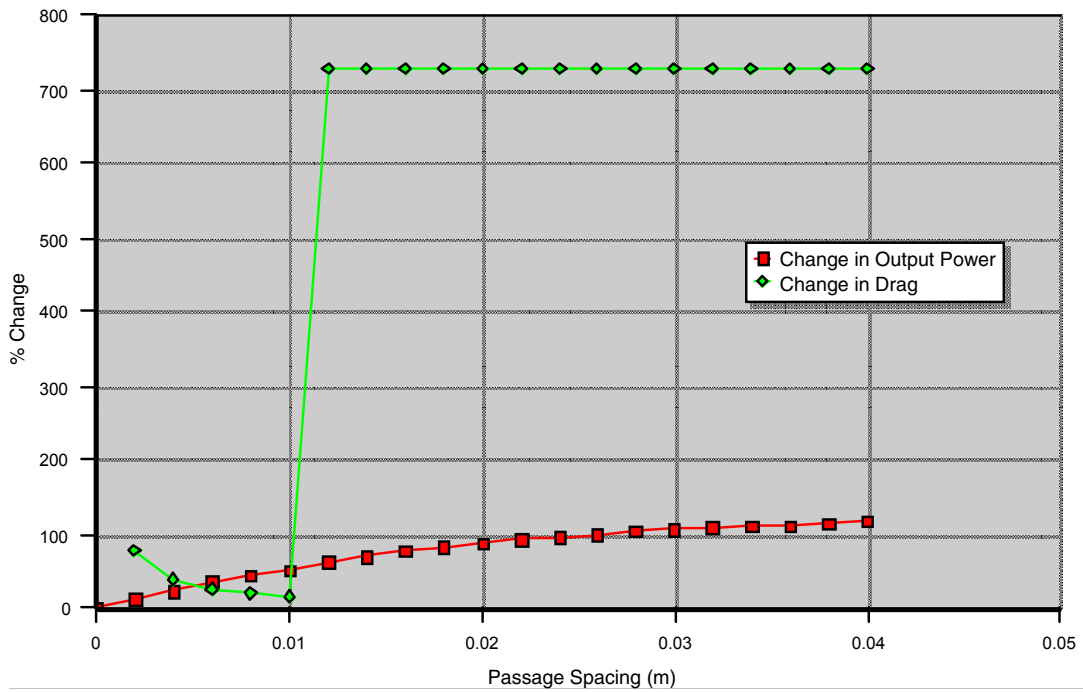


Figure 11.—Percent Change in Solar Cell Performance and Drag.

Based on Figures 10 and 11, the drag of the aircraft increases significantly when the passage spacing is increased beyond 0.01 m. This is for an aircraft wing chord length of 1 m. This is due the transition from laminar to turbulent flow within the cooling passage. Once this transition occurs the percent change in drag is significantly greater than the percent change in array output power. Therefore, beyond this point, it would not be beneficial to utilize the cooling passage to increase the array performance since the additional power generated would not be capable of offsetting the additional drag of the aircraft. Based on these results, the passage spacing of 0.01 m was chosen as the optimal passage spacing for this particular airfoil and aircraft configuration. All of the following results will be based on this cooling passage spacing of 0.01 m.

Utilizing the airfoil shape given in equation 29 and the airfoil and solar cell dimensions given in Table 1, the operating temperature of each cell can be determined for the base flight conditions. These temperatures are shown in Figure 12. This operating temperature was based on heat transfer out of the solar cell as described in the previous section. The main mechanism was the convective heat transfer, which is based on the convective heat transfer coefficient for both the upper surface of the wing and the channel. For the base case, the wing surface convective coefficient was determined to be  $5.23 \text{ W/m}^2 \text{ }^\circ\text{K}$ . For the channel, it was a function of Reynolds number and is given in Figure 13.

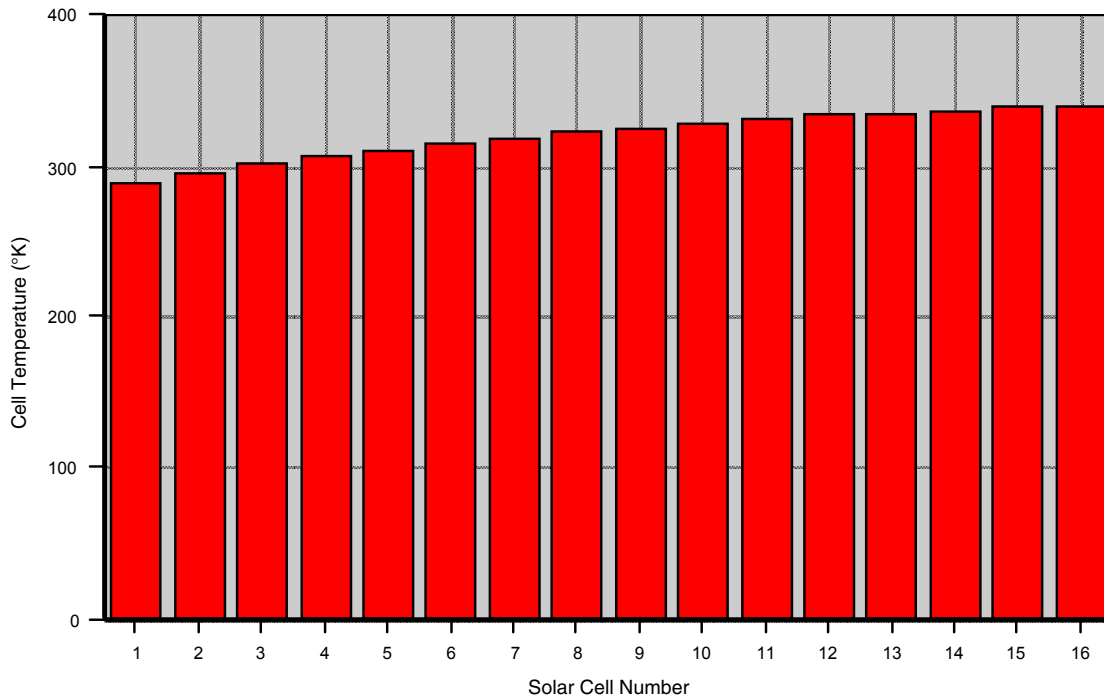


Figure 12.—Solar Cell Temperature.

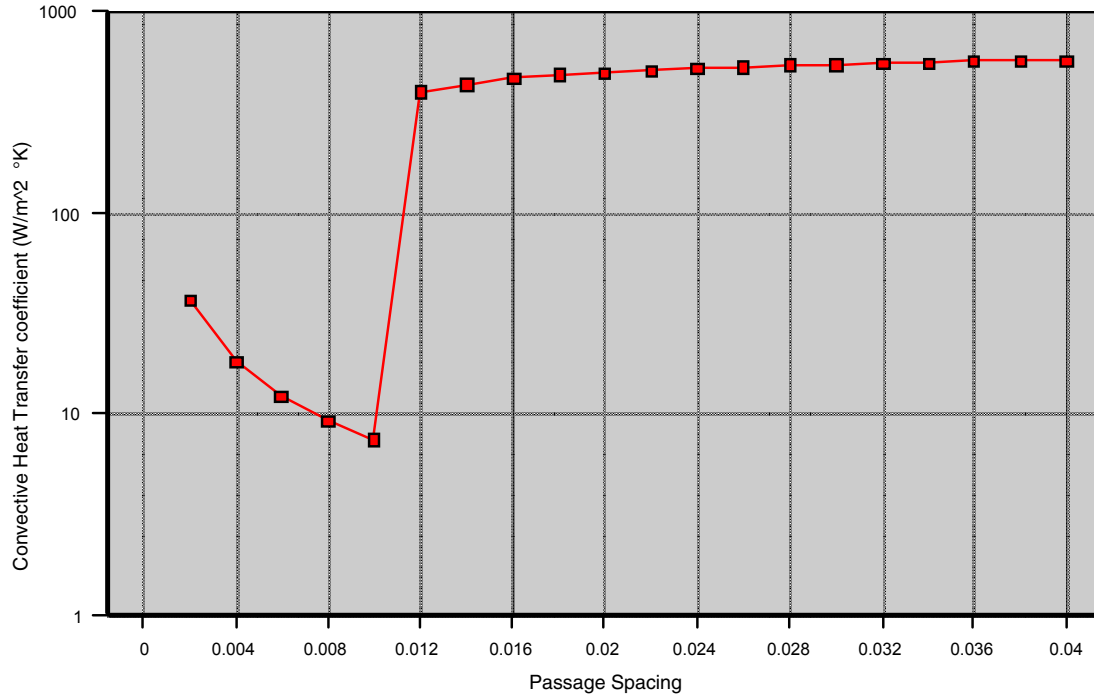


Figure 13.—Relationship Between Passage Spacing and Convective Heat Transfer Coefficient.

The effect of the cooling passage for the base case conditions, given in Table 1, with the optimal cooling passage spacing, 0.01 m, is shown in Figure 14. From this figure it can be seen that there is a significant increase in output power throughout a majority of the day-time period. The dip in the curve for the case without the cooling passage near midday is due to the increased solar cell temperature during operation. This dip is eliminated with the addition of the cooling passage.

The type and characteristics of the solar cell used impacts the overall output performance. However, based on the information given in Figure 3, the change in cell performance for a given temperature change is fairly consistent for all the cell types shown. This change is approximately 3 percent increase in efficiency for a 50 °C change in temperature. Another aspect of the solar cell that influences its operating temperature is the reflection of light off its surface. For a Silicon cell this is given in Figure 7. This reflection versus incident angle depends on the cell material and whatever anti-reflective coating is applied to its surface. Since the reflectance of the cell can be significantly reduced by the application of the anti-reflective coating, the variation in cell reflectivity for different types of solar cells should be minimal. Therefore, the analysis was performed for only Silicon solar cells. Based on the data given in Figure 3 and the anti-reflective coating properties, the results for other cell types should be similar.

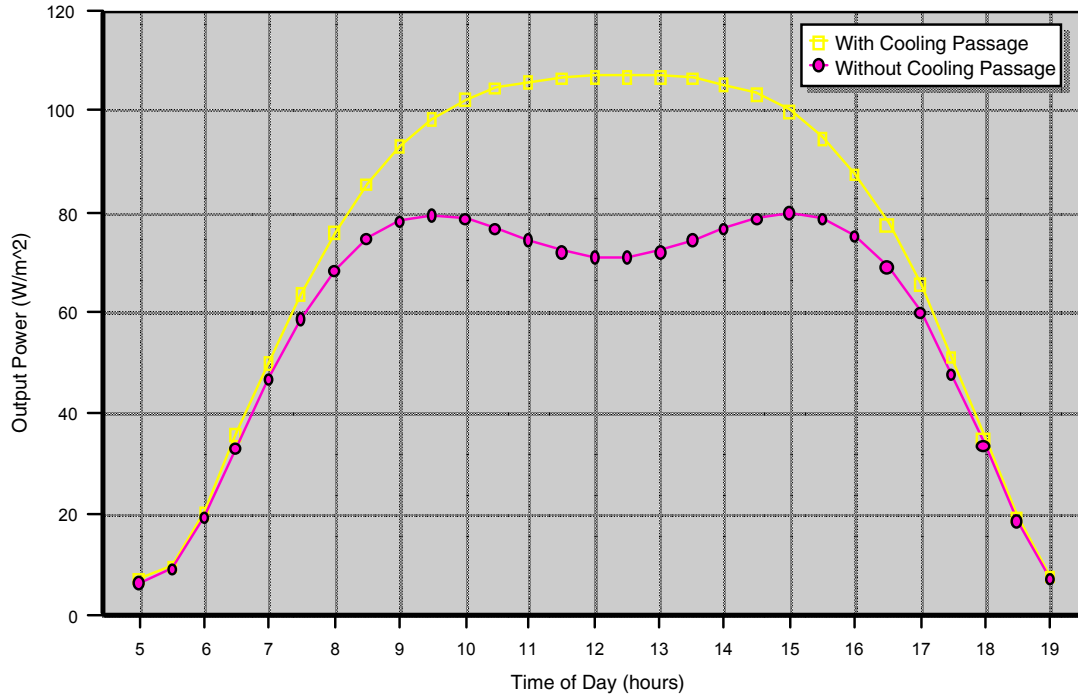


Figure 14.—Solar Cell Output Power Throughout the Daytime Period with and without the Cooling Passage.

The analysis was performed for only one airfoil, the NACA 0009, a symmetrical thin airfoil. The use of a different airfoil would change the results somewhat due to the difference in surface shape and thereby solar cell angle. However, the general performance benefit should be similar for other airfoils since the amount of energy falling on a wing of given chord length is constant regardless of the airfoil shape. The examination of different airfoils was not needed in order to determine the overall feasibility of the cooling passage. In general, the benefits seen in this analysis with the NACA 0009 airfoil should be similar to results with other airfoils. Due to this thin nearly flat airfoil geometry, the variation in performance with orientation of the airfoil was minimal. The solar cell performance was nearly identical for the four orientations examined (North, South, East and West). The data, both with and without the cooling passage, followed very closely the curves shown in Figure 14 for the solar cell performance.

The effect of the cooling passage on the power generated during flight at different latitudes and time of the year are shown in Figures 15 and 16. Since a change in flight latitude or date does not effect the Reynolds number of the flow through the cooling passage, the optimized passage spacing is the same for all latitudes.

From Figure 15 it can be seen that the addition of the cooling passage has the greatest impact on the array output during the midday hours, and little effect during the morning and evening hours. At high latitudes where the sun elevation angle is low, there is a peak increase of approximately 25 percent in array output. This is for the 60° case shown in Figure 14. However, for lower latitudes, such as the 20° case shown, the



increase in midday output power is much more significant, an approximate 60 percent increase in output power. Therefore, from this figure it can be seen that the benefits of the cooling passage are greater at lower latitudes.

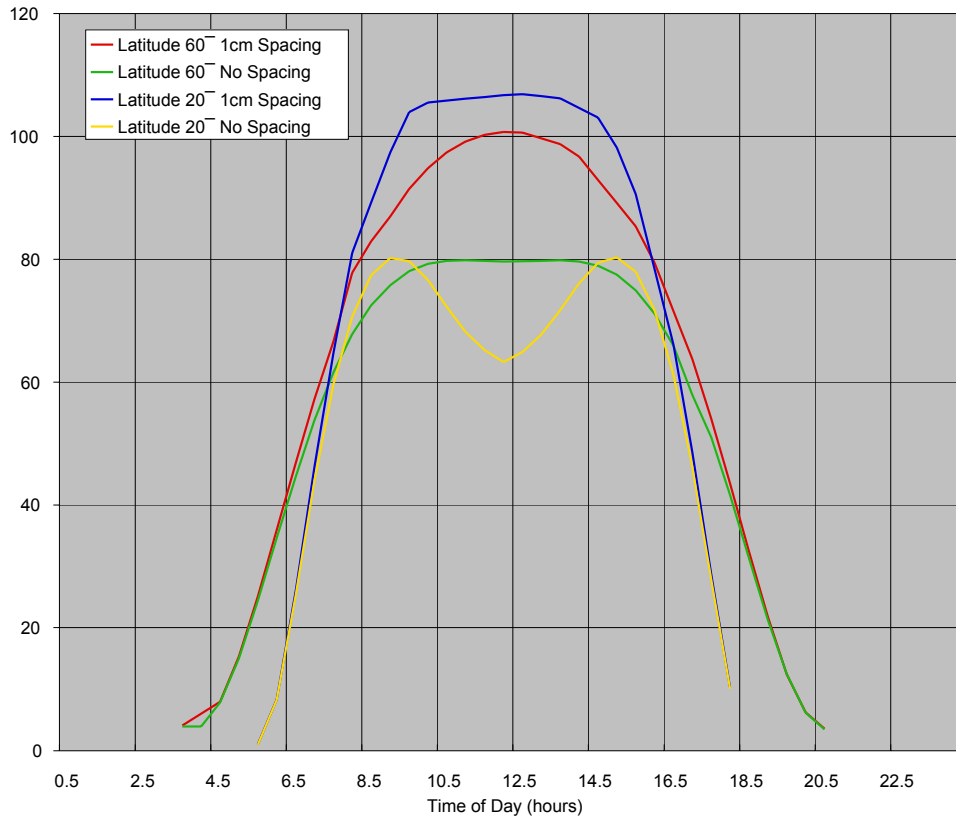


Figure 15.—Effect of Cooling Passage at Various Latitudes.

Figure 16 shows the effect the cooling passage has on the output power, at a given latitude ( $40^{\circ}$  N), at different times of the year. The dates shown are for June 21st and December 21st. These are the two extremes in solar elevation angle. Output power curves for all other dates will fall between these two sets of curves for the same latitude. From this figure it can be seen that the effect on the cooling passage on the output power reaches a peak, at the summer solstice, increasing output power about 54 percent. This effect diminishes to about a 12 percent increase in output power during the winter solstice. This figure demonstrates that at higher sun angles the effect of the cooling passage increases.

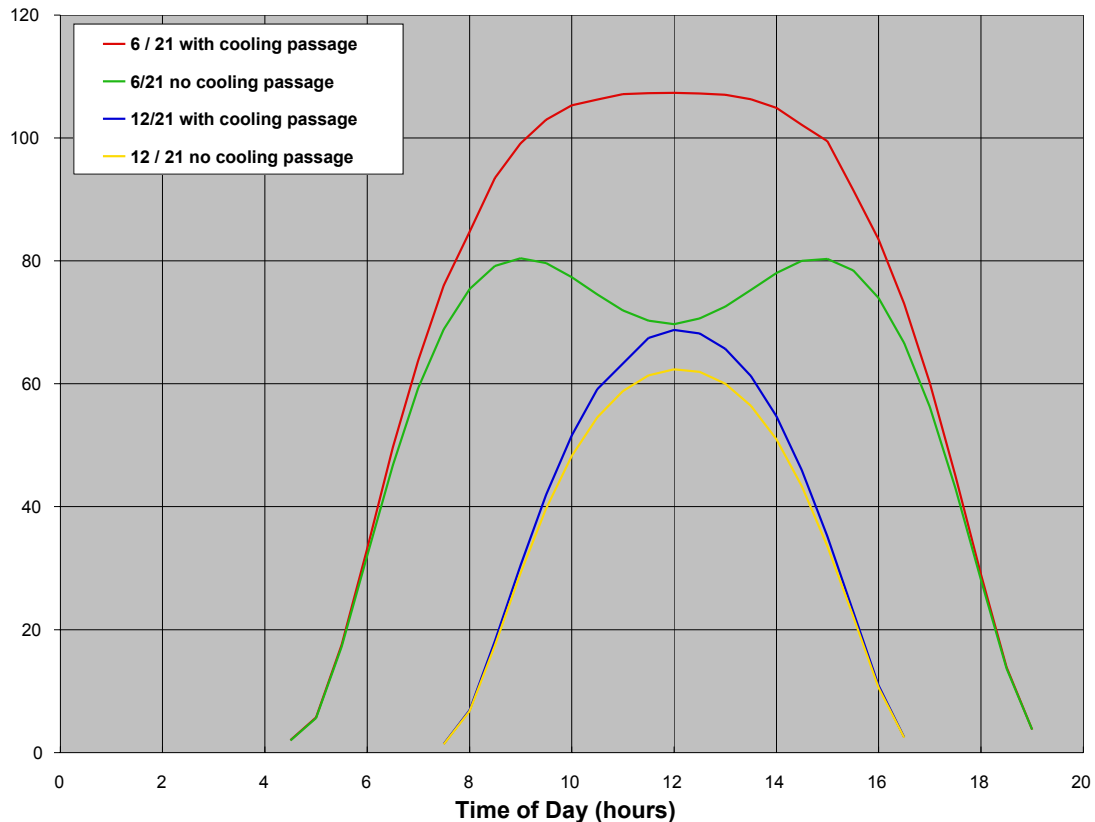


Figure 16.—Solar Array Output at Various Times of the Year.

## References

1. AeroVironment, Inc., ERAST Data Memo, "Pathfinder Flight Test 95-3 Qualitative Report," September 22, 1996.
2. Dornheim, M.A., "Solar-Powered Aircraft Exceeds 50,000 ft," Aviation Week and Space Technology, September 18, 1996.
3. Hall, D.W., Fortenbach, C.D., Dimiceli, E.V., and Parks, R.W., "A Preliminary Study of Solar Powered Aircraft and Associated Power Trains," Lockheed Missiles and Space Company Inc., NASA CR-3699, 1983.
4. Colozza, A.J., "Effect of Power System Technology and Mission Requirements on High Altitude Long Duration Aircraft," NASA CR-194455, February 1994.
5. Lamp, T.R., Reinhardt, K.C., and Colozza, A.J., "Photovoltaic Power for Long Endurance Unmanned Aerial Vehicles," Aero Propulsion and Power Directorate, Wright Laboratory Wright-Patterson AFB Report, 1997.
6. Scheiman, D.A., Jenkins, P.P., Brinker, D.J., and Appelbaum, J., "Low Intensity Low Temperature (LILT) Measurements and Coefficients on New Photovoltaic Structures," SPRAT XIV, Oct. 1995, Progress in Photovoltaics, John Wiley and Sons, Inc. Publisher, March-April, Vol. 4, 1996.
7. Incropera, F.P. and DeWitt, D.P., Fundamentals of Heat and Mass Transfer, John Wiley and Sons, Inc. Publisher, 1990.

8. Scheiman, D.A., Brinker, D.J., Bents, D.J., and Colozza, A.J., "Design of a GaAs/Ge Solar Array for Unmanned Aerial Vehicles," NASA TM-106870, March 1995.
9. Colozza, A.J., Scheiman, D.A. and Brinker, D.J., "GaAs/Ge Solar Powered Aircraft," NASA CR (presently under publication) May 1998.
10. White, F.M., Fluid Mechanics, McGraw Hill Publisher, 1979.
11. Colozza, A.J., "Effect of Date and Location on Maximum Achievable Altitude for a Solar Powered Aircraft," NASA CR-202326, November 1996.
12. Duffie and Beckman, Solar Engineering of Thermal Processes, John Wiley and Sons, Inc. Publisher, 1991.
13. Handbook of tables for Applied Engineering Science, 2nd Edition, CRC Press, 1973.

<b>REPORT DOCUMENTATION PAGE</b>			<i>Form Approved</i> <i>OMB No. 0704-0188</i>	
Public reporting burden for this collection of information is estimated to average 1 hour per response, including the time for reviewing instructions, searching existing data sources, gathering and maintaining the data needed, and completing and reviewing the collection of information. Send comments regarding this burden estimate or any other aspect of this collection of information, including suggestions for reducing this burden, to Washington Headquarters Services, Directorate for Information Operations and Reports, 1215 Jefferson Davis Highway, Suite 1204, Arlington, VA 22202-4302, and to the Office of Management and Budget, Paperwork Reduction Project (0704-0188), Washington, DC 20503.				
<b>1. AGENCY USE ONLY (Leave blank)</b>		<b>2. REPORT DATE</b> January 2003	<b>3. REPORT TYPE AND DATES COVERED</b> Final Contractor Report	
<b>4. TITLE AND SUBTITLE</b>  Convective Array Cooling for a Solar Powered Aircraft			<b>5. FUNDING NUMBERS</b>  WBS-22-708-87-11 NAS3-00145	
<b>6. AUTHOR(S)</b>  Anthony J. Colozza				
<b>7. PERFORMING ORGANIZATION NAME(S) AND ADDRESS(ES)</b>  Analex Corporation 3001 Aerospace Parkway Brook Park, Ohio 44142			<b>8. PERFORMING ORGANIZATION REPORT NUMBER</b>  E-13737	
<b>9. SPONSORING/MONITORING AGENCY NAME(S) AND ADDRESS(ES)</b>  National Aeronautics and Space Administration Washington, DC 20546-0001			<b>10. SPONSORING/MONITORING AGENCY REPORT NUMBER</b>  NASA CR-2003-212084	
<b>11. SUPPLEMENTARY NOTES</b>  Project Manager, James Dolce, Power and On-Board Propulsion Technology Division, NASA Glenn Research Center, organization code 5450, 216-433-8052.				
<b>12a. DISTRIBUTION/AVAILABILITY STATEMENT</b>  Unclassified - Unlimited Subject Categories: 07 and 34 Available electronically at <a href="http://gltrs.grc.nasa.gov">http://gltrs.grc.nasa.gov</a> This publication is available from the NASA Center for AeroSpace Information, 301-621-0390.			<b>12b. DISTRIBUTION CODE</b>	
<b>13. ABSTRACT (Maximum 200 words)</b>  A general characteristic of photovoltaics is that they increase in efficiency as their operating temperature decreases. Based on this principal, the ability to increase a solar aircraft's performance by cooling the solar cells was examined. The solar cells were cooled by channeling some air underneath the cells and providing a convective cooling path to the back side of the array. A full energy balance and flow analysis of the air within the cooling passage was performed. The analysis was first performed on a preliminary level to estimate the benefits of the cooling passage. This analysis established a clear benefit to the cooling passage. Based on these results a more detailed analysis was performed. From this cell temperatures were calculated and array output power throughout a day period were determined with and without the cooling passage. The results showed that if the flow through the cooling passage remained laminar then the benefit in increased output power more than offset the drag induced by the cooling passage.				
<b>14. SUBJECT TERMS</b>  Solar powered aircraft; Solar arrays			<b>15. NUMBER OF PAGES</b> 29	
			<b>16. PRICE CODE</b>	
<b>17. SECURITY CLASSIFICATION OF REPORT</b> Unclassified	<b>18. SECURITY CLASSIFICATION OF THIS PAGE</b> Unclassified	<b>19. SECURITY CLASSIFICATION OF ABSTRACT</b> Unclassified	<b>20. LIMITATION OF ABSTRACT</b>	



